

Effect of BaTiO₃ addition on the microstructure and relaxor ferroelectric properties of Sr_{0.7}Ba_{0.3}Nb₂O₆ ceramics

Jinglei Li*, Yongping Pu, Zhuo Wang, Jie Dai

School of Materials Science and Engineering, Shaanxi University of Science and Technology, Shaanxi Xi'an 710021, China

Received 12 April 2012; received in revised form 17 May 2012; accepted 20 May 2012

Available online 26 May 2012

Abstract

A conventional solid-state reaction was used to synthesize (1- x) Sr_{0.7}Ba_{0.3}Nb₂O₆- x BaTiO₃ (0.00 $\leq x \leq$ 0.10) ceramics. The phase structure, microstructure, and dielectric and relaxor ferroelectric properties of these ceramics were investigated. Tungsten bronze structure can be observed in ceramics, and addition of BaTiO₃ can make the grain size decrease and the porosity increase. The dielectric characteristics show diffuse phase transition phenomena for all samples, which were demonstrated by a linear fit of the modified Curie-Weiss law with γ varying between 1.54 and 1.88. As the BaTiO₃ content increases, the transition temperature (T_C) decreases gradually and has a minimum value of 37.53 °C at composition $x=0.06$, and the maximum dielectric constant (ϵ_{max}) increases gradually from 66 to 3309 and subsequently decreases to 1625 at $x=0.10$. In addition, the relaxor ferroelectric properties of these ceramics at $x=0.8$ are consistent with the Vogel-Fulcher relationship; polarization versus electric field (P - E) loops were measured at a different temperature. © 2012 Elsevier Ltd and Techna Group S.r.l. All rights reserved.

Keywords: Relaxor ferroelectric; Dielectric properties; Curie-Weiss law; Vogel-Fulcher relationship

1. Introduction

The sheer number of studies carried out on relaxor ferroelectrics over the past several years demonstrates the great interest in these materials, both on a theoretical level and for applications. A large, temperature-stable dielectric constant and high electrical resistivity are necessary for developing high-energy density capacitors, which are used in power electric applications, such as filtering, voltage smoothing, dc blocking, power conditioning, electromagnetic interference suppression, and commutation in power electronic circuits. The best-known relaxors are lead-based ceramics, i.e., Pb (Mg_{1/3}Nb_{2/3}) O₃ (PMN) and derived compounds with perovskite structure. In accordance with environmental concerns and to avoid problems related to use of Pb, researchers have moved toward using lead-free relaxors. Among these relaxors, the compositions belonging to either perovskite or tungsten bronze structural families have shown desirable relaxor properties [1–4]. However, most lead-free relaxors

with perovskite structure are characterized by transition temperatures (T_m) below 270 K, as opposed to those with tungsten bronze structures [5–18]. Interestingly, Sr_{0.7}Ba_{0.3}Nb₂O₆ ceramics have a high T_C [19,20]. Previously, we found that compositions of Sr _{x} Ba_{1- x} Nb₂O₆ (0 $\leq x \leq$ 1) have a relaxor effect due to A-site cation disorder when 0.5 $\leq x$. Moreover, Sr_{0.7}Ba_{0.3}Nb₂O₆ displays remarkable relaxor behavior because it meets the high temperature-stable dielectric constant requirement.

The aim of this study is to find lead-free ceramics with transition temperatures above room temperature and to induce relaxor behavior. Also of interest is what would happen when Sr_{0.7}Ba_{0.3}Nb₂O₆, a relaxor ferroelectric, and BaTiO₃, a ferroelectric, form a solid solution. Few reports on the dielectric and relaxor ferroelectric properties of Sr_{0.7}Ba_{0.3}Nb₂O₆ doped with BaTiO₃ have been previously published. The effect of BaTiO₃ doping on phase formation, microstructure, and the dielectric and relaxor ferroelectric properties of Sr_{0.7}Ba_{0.3}Nb₂O₆ ceramics were studied in detail in this study. In addition, polarization versus electric field (P - E) loops of ceramics with composition $x=0.08$ were measured at different temperature.

*Corresponding author. Fax: +86 18792815467.

E-mail address: lilei19871003@yahoo.com.cn (J. Li).

2. Experiment procedure

The compositions belonging to the system $(1-x)$ $\text{Sr}_{0.7}\text{Ba}_{0.3}\text{Nb}_2\text{O}_6$ – $x\text{BaTiO}_3$ ($0.00 \leq x \leq 0.10$) were investigated in this study. The samples were synthesized from reagent-grade SrCO_3 (99.95%), BaCO_3 (99.95%), Nb_2O_5 (99.95%) and TiO_2 (99.5%) powders using conventional solid-state reaction. BaCO_3 and TiO_2 were added to a ball mill jar in stoichiometric proportions and later milled for 2 h in distilled water with ZrO_2 media. After the slurry was dried, a mixture consisting of BaCO_3 and TiO_2 was calcined in an alumina crucible at 1150°C for 3 h in air to form BaTiO_3 powder. The calcined BaTiO_3 powder was milled with varying stoichiometric proportions of SrCO_3 , BaCO_3 and Nb_2O_5 in ZrO_2 media with distilled water for 4 h and dried for 2 h. After adding 5 wt% polyvinyl alcohol (PVA), the powders were dry pressed into disks at a pressure of 10 MPa in a 13.6 mm diameter stainless steel cylindrical die at room temperature. These disks were sintered at 1350°C for 2 h in air to yield dense ceramics. The crystal phase of the sintered ceramics was characterized by powder X-ray diffraction (XRD) analysis with $\text{Cu K}\alpha$ radiation. The surfaces of the disks were polished and thermally etched before observing the microstructure with scanning electron microscopy (SEM; Jeol, JSM-5400). SEM micrographs were taken in randomly selected areas of each specimen. To make a good contact, the disks were fired with conducting silver paste at 600°C for 0.5 h. The dielectric response of the ceramic disks was measured with an Agilent E4980A over temperatures ranging from room temperature to 300°C . Polarization versus electric field (P-E) loops of $x=0.08$ ceramic were measured at different temperatures.

3. Results and Discussion

The XRD patterns of the $(1-x)$ $\text{Sr}_{0.7}\text{Ba}_{0.3}\text{Nb}_2\text{O}_6$ – $x\text{BaTiO}_3$ ($0.00 \leq x \leq 0.10$) ceramics with varying BaTiO_3 content is shown in Fig. 1. The ceramics have a tungsten bronze (TB) structure, and a rare second phase can be detected when $x \geq 0.08$, which indicates that most of the Ba^{2+} and Ti^{4+} ions have diffused into the tungsten bronze lattice structure to form a solid solution. It is generally accepted that $\text{Sr}_x\text{Ba}_{1-x}\text{Nb}_2\text{O}_6$ ($0.25 \leq x \leq 0.75$) ceramics have a TB structure with a unit-cell formula of $\text{A}_1\text{A}_2\text{C}_4\text{B}_1\text{B}_2\text{O}_{30}$, which consists of layers of $[\text{BO}_6]$ corner-sharing octahedra that form three types of interstitial channels: square A1, pentagonal A2, and triangular C channels. The pentagonal and square channels are usually occupied by large alkali, alkaline earth and rare earth cations [21]. In the tetragonal SBN crystal, Sr^{2+} ions (1.12 \AA radius) and Ba^{2+} ions (1.35 \AA radius) occupy the A sites, whereas Nb^{5+} ions (0.64 \AA radius) occupy the B sites and form $[\text{NbO}_6]$ octahedra with six oxygen atoms [22]. In addition, it is reasonable to assume that Ti^{4+} ions can substitute for Nb^{5+} ions, as their valence states and ionic radii are similar.

Fig. 2 shows SEM micrographs of ceramics with compositions of $x=0.00$, 0.04, 0.08, and 0.10 sintered at

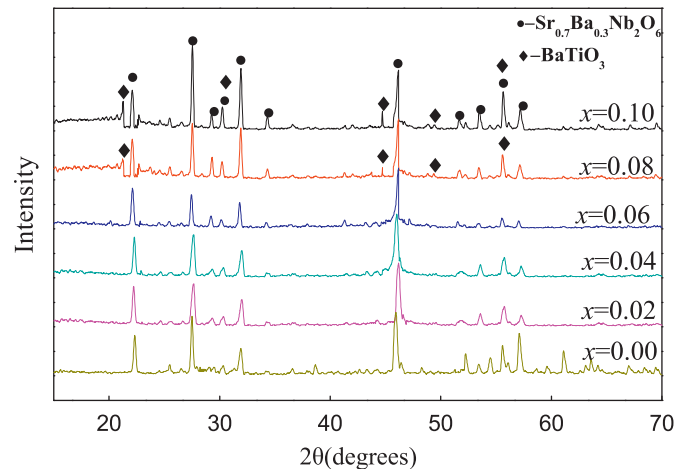


Fig. 1. XRD patterns of $(1-x)$ $\text{Sr}_{0.7}\text{Ba}_{0.3}\text{Nb}_2\text{O}_6$ – $x\text{BaTiO}_3$ ($0.00 \leq x \leq 0.10$) ceramics as a function of composition x .

1350°C . It can be observed in Fig. 2 that the addition of BaTiO_3 to $\text{Sr}_{0.7}\text{Ba}_{0.3}\text{Nb}_2\text{O}_6$ decreases the grain size and increases the porosity.

Fig. 3 shows the temperature dependence of the dielectric constant of ceramics with composition $0 \leq x \leq 0.10$ at different frequencies. Several broad dielectric peaks are observed in the samples, which indicate ferroelectric phase transitions. The positions of the maximum dielectric constant shift toward higher temperatures as the frequency increases; this phenomenon is indicative of relaxor behavior. The data are consistent with the relaxor ferroelectric nature of ceramic solutions, which could arise from local compositional disorders of Sr^{2+} and Ba^{2+} in the A1 and A2 sites [19,23,24]. In the tungsten bronze structure, the A1 sites are occupied by Sr^{2+} only, and the A2-sites are filled with both Sr^{2+} and Ba^{2+} , whereas the C channels remain empty. As there are only five Sr and Ba atoms for the six A1 and A2 positions, one of the A sites remains unoccupied; the missing charge in these vacancies is the source of random fields (RFs) [25]. In addition, occupation of A2 sites by different cations creates disorder in the oxygen ion positions, due to the difference between Ba–O and Sr–O bonding lengths. Therefore, the disorder of ions in the unit cell should be the reason for the appearance of the frequency dispersion.

Fig. 4 shows the temperature dependence of the dielectric constant of ceramics with composition $0.00 \leq x \leq 0.10$. The dielectric constant increases with temperature up to the transition temperature (T_C) and later decreases with increasing temperatures above T_C , which is normal behavior for ferroelectrics. The peaks observed are associated with a ferroelectric tetragonal to para-electric cubic phase transition.

Fig. 5 shows the phase transition temperature (Curie temperature T_C) and the maximum dielectric constant (ϵ_{max}) of ceramics with composition $0.00 \leq x \leq 0.10$. The maximum dielectric constant ϵ_{max} increases gradually from 66 to 3309 with increasing x and later decreases to 1625 at

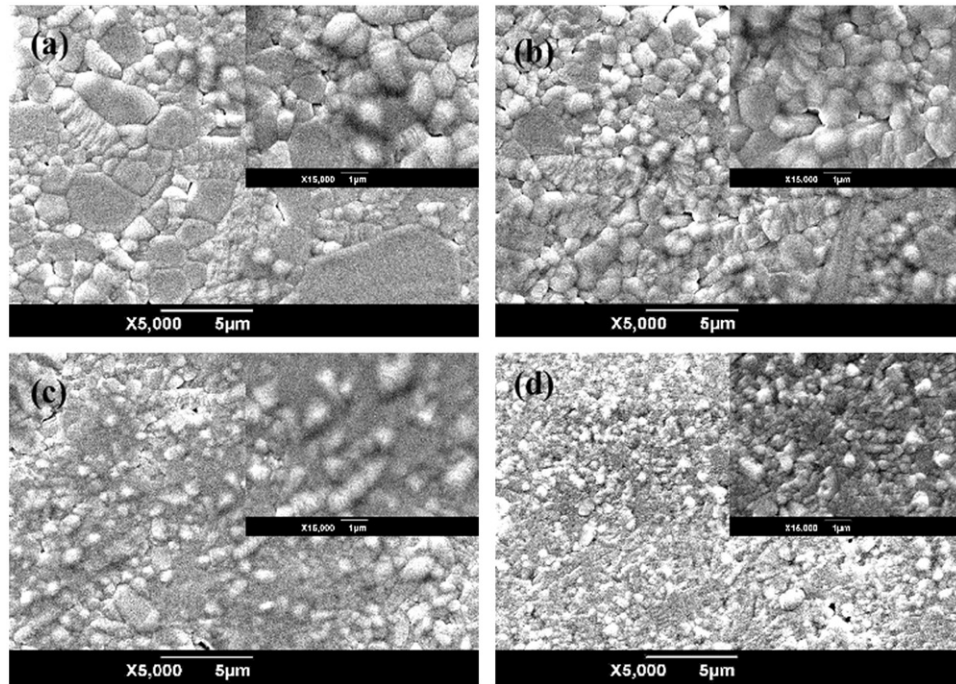


Fig. 2. SEM micrographs of $(1-x)$ $\text{Sr}_{0.7}\text{Ba}_{0.3}\text{Nb}_2\text{O}_6-x\text{BaTiO}_3$ ($0.00 \leq x \leq 0.10$) ceramics sintered at 1350°C : (a) $x=0.00$, (b) $x=0.04$, (c) $x=0.08$, (d) $x=0.10$.

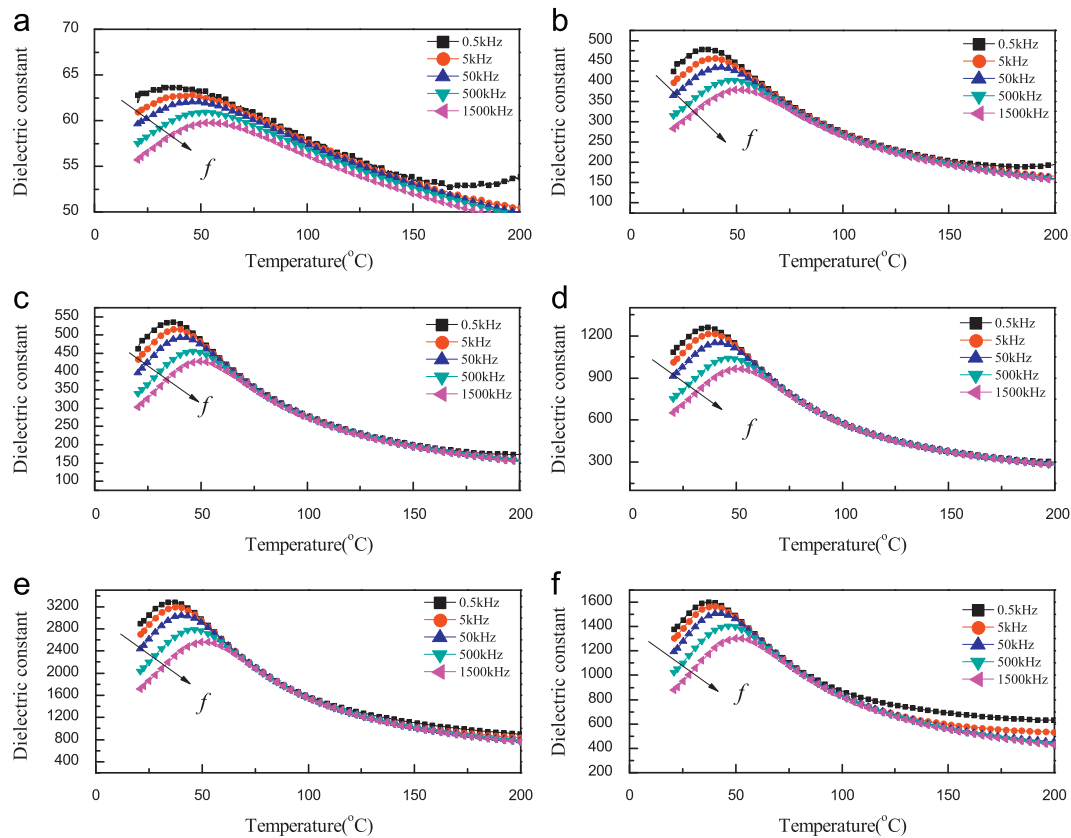


Fig. 3. Temperature dependence of the dielectric constant of $(1-x)$ $\text{Sr}_{0.7}\text{Ba}_{0.3}\text{Nb}_2\text{O}_6-x\text{BaTiO}_3$ ($0.00 \leq x \leq 0.10$) ceramics at different frequencies: (a) $x=0.00$, (b) $x=0.02$, (c) $x=0.04$, (d) $x=0.06$, (e) $x=0.08$, (f) $x=0.10$.

$x=0.10$, whereas T_C has an opposite trend with ϵ_{max} and has a minimum value of 37.53°C at $x=0.06$. The decrease in T_C may be due to an increase in Ti^{4+} substitution for

Nb^{5+} ions, whereas the increase in T_C may be due to an increase in Ba^{2+} ions among the $[\text{NbO}_6]$ octahedra in the pentagonal channel. The increased concentration of Ba^{2+}

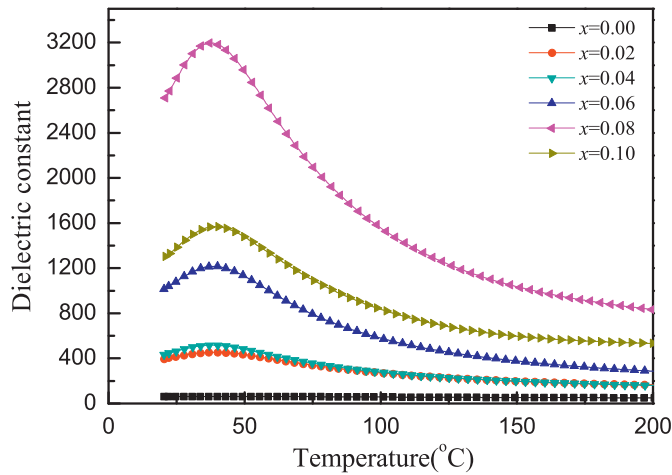


Fig. 4. Temperature dependence of dielectric constant of $(1-x)$ $\text{Sr}_{0.7}\text{Ba}_{0.3}\text{Nb}_2\text{O}_6-x\text{BaTiO}_3$ ($0.00 \leq x \leq 0.10$) ceramics.

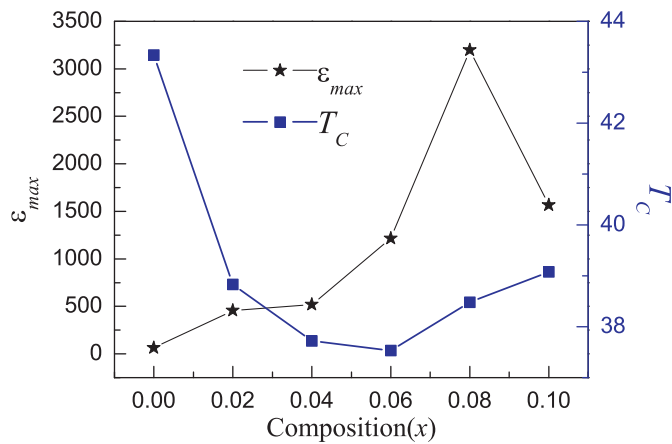


Fig. 5. T_C and ϵ_{\max} of $(1-x)$ $\text{Sr}_{0.7}\text{Ba}_{0.3}\text{Nb}_2\text{O}_6-x\text{BaTiO}_3$ ($0.00 \leq x \leq 0.10$) ceramics as a function of composition x .

ions means that there are fewer Sr^{2+} ions among the $[\text{NbO}_6]$ octahedra because the $[\text{NbO}_6]$ octahedra cannot accommodate distortions from Sr^{2+} as easily, given that the Sr-O electron cloud overlaps more so than that of Ba-O, thereby increasing the potential energy of the oxygen atoms. Therefore, T_C decreases gradually and later increases with the increasing x .

The broad dielectric peaks illustrate behavior typical of relaxors in which the dielectric constant decreases and the maximum dielectric constant temperature T_C shifts to high temperature with an increase in frequency, indicating a diffuse phase transition (DPT). The DPT can be described by modified Curie-Weiss law [26–28]:

$$\frac{1}{\epsilon} - \frac{1}{\epsilon_{\max}} = \frac{(T - T_C)^\gamma}{C}, \quad (1)$$

where ϵ is the dielectric constant, T is the temperature, ϵ_{\max} is the maximum ϵ value at $T = T_C$, C is the modified Curie-Weiss constant and γ is a measurement of diffusivity, the materials with $\gamma = 1$ fit normal ferroelectric behavior, with

$\gamma = 2$ showing a complete disordered system, and between 1 and 2 indicating diffuse ferroelectric characteristics.

Fig. 6 shows the relationship between $\ln(1/\epsilon - 1/\epsilon_{\max})$ and $\ln(T - T_C)$ of ceramics with composition $0.00 \leq x \leq 0.10$. The diffuse exponent γ increases gradually from 1.54764 to 1.87693 with the increasing x and subsequently decreases to 1.78978 at $x = 0.10$. The diffuse exponents of ceramics with composition $0.02 \leq x \leq 0.10$ are all close to 2, which is consistent with typical diffuse ferroelectric behavior [29]. In addition, this γ value has also been observed in other tungsten bronze compounds [30]. Further investigation was needed to explain this phenomenon and a ceramic composition $x = 0.08$ was chosen due to its high dielectric constant and having the largest diffuse exponent, as observed in Figs. 5 and 6. The frequency dependence of T_C is found to obey the Vogel-Fulcher relationship closely [31,32]:

$$f = f_0 e^{-E_a/K_B(T_C - T_f)}, \quad (2)$$

where f_0 is a pre-exponential term, E_a is the activation energy for polarization fluctuation of an isolated micro-polar region, T_C is the temperature of the dielectric constant maximum, E_B is the Boltzmann constant, and T_f is the Vogel–Fulcher temperature, i.e., the static freezing temperature.

Fig. 7 shows the temperature dependence of the dielectric constant at different frequencies and the inverse of Curie temperature T_C as a function of measurement frequency for ceramics with composition $x = 0.08$. The fitting parameters were obtained as $E_a = 0.0042$ eV, $T_f = 302.36$ K, $f_0 = 1.21 \times 10^7$ Hz. This finding indicates that ceramics with composition $x = 0.08$ have typical spun-glass-like dielectric relaxation behavior. This glassy behavior is believed to originate from the randomly oriented dipolar and electric fields between phase-separated super-para-electric moments [33].

Fig. 8 shows the P - E loops measured at various temperature of ceramics with composition $x = 0.08$. Saturated P - E loops have almost constant Pr values at different temperatures.

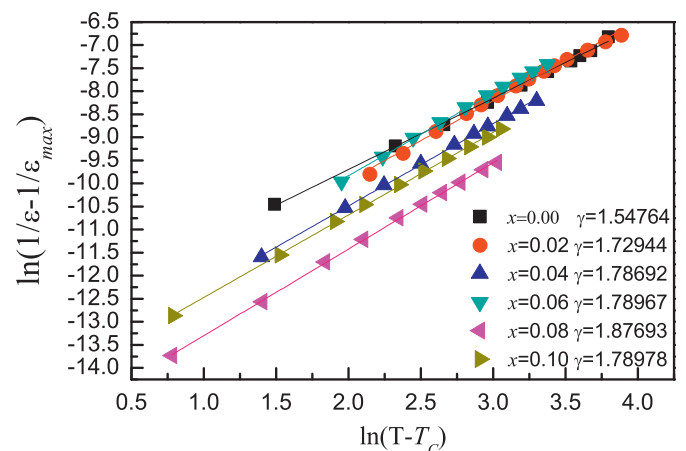


Fig. 6. Relationship between $\ln(1/\epsilon - 1/\epsilon_{\max})$ and $\ln(T - T_C)$ of $(1-x)$ $\text{Sr}_{0.7}\text{Ba}_{0.3}\text{Nb}_2\text{O}_6-x\text{BaTiO}_3$ ($0.00 \leq x \leq 0.10$) ceramics.

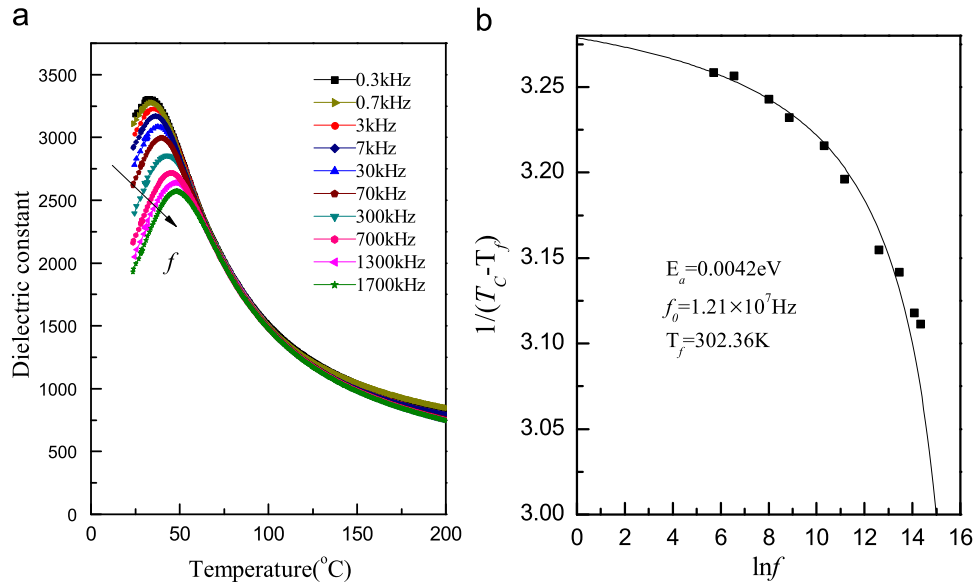


Fig. 7. (a) Temperature dependence of the dielectric constant of ceramics with composition $x=0.08$ at different frequencies. (b) Inverse of Curie temperature T_C as a function of the measurement frequency of ceramics with composition $x=0.08$.

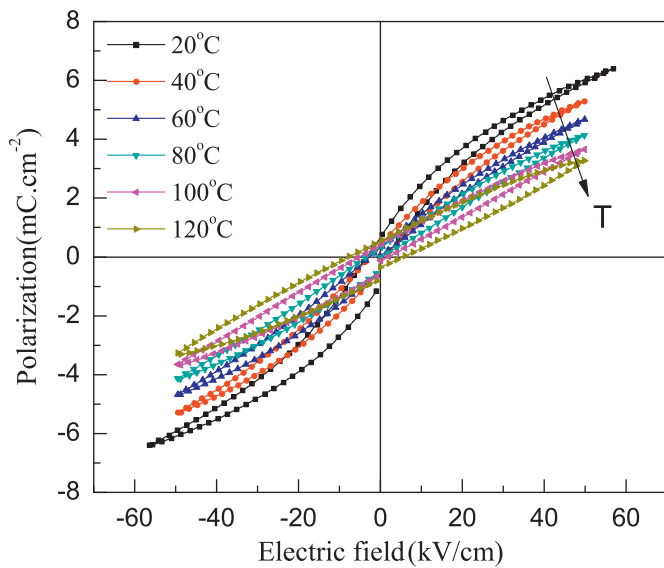


Fig. 8. Polarization versus electric field (P - E) loops of ceramics with composition $x=0.08$ at different temperatures.

As the measurement temperature increases, the P_s values decrease, and the P - E loops gradually become wider, but there still exists a nonlinear P - E loop, even when the measured temperature is above T_C , which implies the existence of polar nano-micro-regions [34].

4. Conclusions

Tungsten bronze structure $\text{Sr}_{0.7}\text{Ba}_{0.3}\text{Nb}_2\text{O}_6$ ceramics doped with BaTiO_3 were prepared by the conventional mixed-oxide method. The phase structure, microstructure, and dielectric properties and ferroelectric properties of resulting ceramics were investigated as functions of BaTiO_3 content. The results

showed that tungsten bronze structure could be observed, and a rare second phase could be detected in ceramics with composition $x \geq 0.08$. Furthermore, the grain size decreases and the porosity increases with increasing BaTiO_3 content. The dielectric characteristics show diffuse phase transition phenomena for all of the ceramics investigated, which were proved by linear fits to the modified Curie-Weiss law. The maximum dielectric constant (ϵ_{max}) increases gradually from 67 to 3309 and decreases thereafter to 1625 at composition $x=0.10$ with increasing BaTiO_3 content, but T_C has an opposite dependence on ϵ_{max} and has a minimum value of 37.53 °C at composition $x=0.06$. Ceramics with composition $x=0.08$ were chosen for further investigation to explain this phenomenon, due to their high dielectric constant and having the largest diffuse exponent, which has a strong frequency dispersion that agrees well with the Vogel-Fulcher relationship. In addition, saturated P - E loops have almost constant P_r values at different temperatures. With increasing measurement temperature, the P_s values decrease, and the P - E loops gradually become wider, but there still exists a nonlinear P - E loop, even when the measured temperature is above T_C , which implies the existence of polar nano-micro-regions.

Acknowledgments

This research was supported by the National Natural Science Foundation of China (51072106, 51102159), the New Century Excellent Talents Program of Chinese Education Ministry (NCET-11-1042), Foundation of Shaanxi Educational Committee (12JK0447), the International Science and Technology Cooperation Project Funding of Shaanxi Province (2012KW-06), and the Academic Leaders Cultivation Program and Graduate Innovation Fund of Shaanxi University of Science and Technology.

References

- [1] Wan Q. Cao, Li Yang, Mukhlis M. Ismail, Ping Feng, Dielectric and ferroelectric properties of $\text{Ba}_{0.8}\text{Sr}_{0.2}\text{Ti}_{1-5x/4}\text{Nb}_x\text{O}_3$ ceramics, *Ceramics International* 37 (2011) 1587–1591.
- [2] J.G. Cheng, J. Tang, J.H. Chu, A.J. Zhang, Pyroelectric properties in sol-gel derived barium strontium titanate thin films using a highly diluted precursor solution, *Appl. Phys. Lett.* 77 (2001) 1035–1037.
- [3] R.W. Wahore, R. Watton, Pyroelectric ceramics and thin films for uncooled thermal imaging, *Ferroelectrics* 236 (2000) 259–279.
- [4] G.W. Dietz, M. Schumacher, R. Waser, S.K. Streiffer, C. Basceri, A.J. Kingon, Leakage currents in $\text{Ba}_{0.7}\text{Sr}_{0.3}\text{TiO}_3$ thin films for ultrahigh-density dynamic random access memories, *J. Appl. Phys.* 82 (1997) 2359–2364.
- [5] N. Abdelmoula, H. Chaabane, H. Khemakem, R. von der muhl, A. Simon, Relaxor or Classical Ferroelectric Behavior in A-Site Substituted Perovskite Type $\text{Ba}_{1-x}(\text{Sm}_{0.5}\text{Na}_{0.5})\text{TiO}_3$, *Solid State Sci* 8 (2006) 880–887.
- [6] R. Farhi, M.E.I. Marssi, A. Simon, J. Ravez, Relaxor-Like and Spectroscopic Properties of Niobium Modified Barium Titanate, *Eur. Phys. J.* 18 (1999) 605–610.
- [7] H. Ogihara, C.A. Randall, S. Trolier-Mckinstry, Weakly Coupled Relaxor Behavior of BaTiO_3 - BiScO_3 Ceramics, *J. Am. Ceram. Soc.* 92 (2009) 110–118.
- [8] A.N. Salak, M.P. Seabra, V.M. Ferreira, Evolution from Ferroelectric to Relaxor Behavior in the $(1-x)\text{BaTiO}_3$ - $x\text{La}(\text{Mg}_{1/2}\text{Ti}_{1/2})\text{O}_3$ System, *Ferroelectrics* 318 (2005) 185–192.
- [9] H. Khemakem, A. Simon, R. Von der Muhll, J. Ravez, Relaxor or Classical Ferroelectric Behavior in Ceramics with Composition $\text{Ba}_{1-x}\text{Na}_x\text{Ti}_{1-x}\text{Nb}_x\text{O}_3$, *J. Phys.: Condens. Matter* 12 (2000) 5951–5959.
- [10] J. Ravez, A. Simon, Le premier relaxor ferroelectrique oxyfluore, *Phys. Status Solidi A* 184 (2001) 459–494.
- [11] A. Simon, J. Ravez, New Lead-Free Relaxor, Ceramics Derived from BaTiO_3 by Cationic Heterovalent Substitutions in the 12 C.N Crystallographic Site, *Solid State Sci.* 2 (2000) 525–529.
- [12] A. Simon, J. Ravez, M. Maglione, The Crossover from a Ferroelectric to a Relaxor State in Lead-Free Solid Solutions, *J. Phys.: Condens. Matter* 16 (2004) 963–970.
- [13] V.V. Shvartsman, J. Zhai, W. Kleemann, The Dielectric Relaxation in Solid Solutions $\text{BaTi}_{1-x}\text{Zr}_x\text{O}_3$, *Ferroelectrics* 379 (2009) 77–85.
- [14] V.V. Shvartsman, J. Dec, Z.K. Xu, J. Banys, P. Keburis, W. Kleemann, Crossover from Ferroelectric to Relaxor Behavior in $\text{BaTi}_{1-x}\text{Sn}_x\text{O}_3$ Solid Solutions, *Phase Transitions* 81 (2008) 1013–1021.
- [15] T. Lukasiewicz, M.A. Swirkowicz, J. Dec, W. Hofman, W. Szyrski, Strontium-Barium Niobate Single Crystals, Growth and Ferroelectric Properties, *J. Cryst. Growth* 310 (2008) 1464–1469.
- [16] L. Cui, Y.D. Hou, S. Wang, M.K. Zhu, Relaxor Behavior of $(\text{Ba},\text{Bi})(\text{Ti},\text{Al})\text{O}_3$ Ferroelectric Ceramic, *J. Appl. Phys.* 107 (2010) 054105.
- [17] H. Chaabane, N. Avdelmoula, H. Khemakem, A. Simon, D. Michau, M. Maglione, Dielectric and Ferroelectric Properties of Lead-Free $\text{Ba}_{1-x}\text{La}_x\text{Ti}_{1-x}\text{Fe}_x\text{O}_3$ Ceramics, *Phys. Status Solidi A* 208 (2011) 180–185.
- [18] S. Kumar, K.B.R. Varma, Relaxor Behavior of $\text{BaBi}_4\text{TiFe}_{0.5}\text{Nb}_{0.5}\text{O}_{15}$ Ceramics, *Solid State Commun.* 147 (2008) 457–460.
- [19] A.M. Glass, Investigation of the Electrical properties of $\text{Sr}_{1-x}\text{Ba}_x\text{Nb}_2\text{O}_6$ with Special Reference to Pyroelectric Detection, *J. Appl. Phys.* 40 (1996) 4699–4713.
- [20] T. Lukasiewicz, M.A. Swirkowicz, J. Dec, W. Hofman, W. Szyrski, Strontium-Barium Niobate Single Crystals, Growth and Ferroelectric Properties, *J. Cryst. Growth* 310 (2008) 1464–1469.
- [21] Y.J. Wu, S.P. Gu, Y.Q. Lin, Z.J. Hong, X.Q. Liu, X.M. Chen, Multiferroic ceramics in $\text{BaO}-\text{Y}_2\text{O}_3-\text{Fe}_2\text{O}_3-\text{Nb}_2\text{O}_5$ system, *Ceramics International* 36 (2010) 2415–2420.
- [22] P.B. Jamieson, S.C. Abrahams, J.L. Bernstein, Ferroelectric Tungsten Bronze-Type Crystal Structures- Barium Strontium Niobate $\text{Ba}_{0.27}\text{Sr}_{0.73}\text{Nb}_2\text{O}_{5.78}$, *J. Chem. Phys.* 48 (1968) 5048–5057.
- [23] V.V. Shartsman, J. Dec, S. Miga, T. Lukaciewicz, W. Kleemann, Ferroelectric Domains in $\text{Sr}_x\text{Ba}_{1-x}\text{Nb}_2\text{O}_6$ Single Crystals ($0.4 \leq x \leq 0.75$), *Ferroelectrics* 376 (2008) 197–204.
- [24] T.S. Chernaya, B.A. Maksimov, I.V. Versin, L.I. Ivleva, V.I. Simonov, Crystal Structure of $\text{Ba}_{0.39}\text{Sr}_{0.61}\text{Nb}_2\text{O}_6$, *Crystallogr. Rep.* 42 (1997) 375–380.
- [25] A.A. Bokov, Z.G. YE, Recent progress in relaxor ferroelectrics with perovskite structure, *Journal of Materials Science* 41 (2006) 31–52.
- [26] V.V. Kirrillow, V.A. Isupov, Relaxation polarization of $\text{PbMg}_{1/3}\text{Nb}_{2/3}\text{O}_3$ (PMN)-a ferroelectric with a diffused phase transition, *Ferroelectrics* 5 (1973) 3–9.
- [27] Z.R. Liu, Y. Zhang, B.L. Gu, X.W. Zhang, The properties of frozen local polarization in relaxor ferroelectrics, *J. Phys.: Condens. Matter* 13 (2001) 1133–1139.
- [28] K. Uchino, S. Nomura, Critical exponents of the dielectric constant in diffused-phase-transition crystals, *Ferroelectric* 44 (1982) 55–61.
- [29] A. Aoujgal, W.A. Gharbi, A. Outzourhit, A. Ammar, A. Tachafine, J.C. Carru, Relaxor behavior in $(\text{Ba}_{1-3x/2}\text{Bi}_x)(\text{Zr}_y\text{Ti}_{1-y})\text{O}_3$ ceramics, *Ceramics International* 37 (2011) 2069–2074.
- [30] X.L. Zhu, X.M. Chen, X.Q. Liu, Dielectric abnormality of $\text{Sr}_4\text{Nd}_2\text{Ti}_4\text{Nb}_6\text{O}_{30}$ tungsten bronze ceramics over a broad temperature range, *J. Mater. Res.* 22 (2007) 2217–2222.
- [31] H. Vogel, The law of the relation between the viscosity of liquids and the temperature, *Phs. Zeit* 22 (1921) 645–646.
- [32] G.S. Fulcher, Analysis of recent measurements of the viscosity of glasses, *J. Am. Ceram. Soc* 8 (1925) 339–355.
- [33] M. Adamczyk, A. Molak, Z. Ujma, The influence of axial pressure on relaxor properties of $\text{BaBi}_2\text{Nb}_2\text{O}_9$ ceramics, *Ceramics International* 35 (2009) 2197–2202.
- [34] S. Wongsanmai, S. Ananta, X. Tan, R. Yimnirun, Dielectric and ferroelectric properties of lead indium niobate ceramic prepared by wolframite method, *Ceramics International* 34 (2008) 723–726.